

The Role of Ocean Tides on Groundwater-Surface Water Exchange in a Mangrove-Dominated Estuary: Shark River Slough, Florida Coastal Everglades, USA

Christopher G. Smith¹ · René M. Price² · Peter W. Swarzenski³ · Jeremy C. Stalker⁴

Received: 21 July 2015 / Revised: 2 February 2016 / Accepted: 5 February 2016
© Coastal and Estuarine Research Federation (outside the USA) 2016

Abstract Low-relief environments like the Florida Coastal Everglades (FCE) have complicated hydrologic systems where surface water and groundwater processes are intimately linked yet hard to separate. Fluid exchange within these low-hydraulic-gradient systems can occur across broad spatial and temporal scales, with variable contributions to material transport and transformation. Identifying and assessing the scales at which these processes operate is essential for accurate evaluations of how these systems contribute to global biogeochemical cycles. The distribution of ^{222}Rn and $^{223,224,226}\text{Ra}$ have complex spatial patterns along the Shark River Slough estuary (SRSE), Everglades, FL. High-resolution time-series measurements of ^{222}Rn activity, salinity, and water level were used to quantify processes affecting radon fluxes out of the mangrove forest over a tidal cycle. Based on field data, tidal

pumping through an extensive network of crab burrows in the lower FCE provides the best explanation for the high radon and fluid fluxes. Burrows are irrigated during rising tides when radon and other dissolved constituents are released from the mangrove soil. Flushing efficiency of the burrows—defined as the tidal volume divided by the volume of burrows—estimated for the creek drainage area vary seasonally from 25 (wet season) to 100 % (dry season) in this study. The tidal pumping of the mangrove forest soil acts as a significant vector for exchange between the forest and the estuary. Processes that enhance exchange of O_2 and other materials across the sediment-water interface could have a profound impact on the environmental response to larger scale processes such as sea level rise and climate change. Compounding the material budgets of the SRSE are additional inputs from groundwater from the Biscayne Aquifer, which were identified using radium isotopes. Quantification of the deep groundwater component is not obtainable, but isotopic data suggest a more prevalent signal in the dry season. These findings highlight the important role that both tidal- and seasonal-scale forcings play on groundwater movement in low-gradient hydrologic systems.

Communicated by Isaac Santos

Electronic supplementary material The online version of this article (doi:10.1007/s12237-016-0079-z) contains supplementary material, which is available to authorized users.

✉ Christopher G. Smith
cgsmith@usgs.gov

¹ USGS St. Petersburg Coastal and Marine Science Center, 600 Fourth Street South, St. Petersburg, FL 33701, USA

² Department of Earth and Environment and Southeast Environmental Research Center, Florida International University, AHC5-373, 11200 S.W. 8th St., Miami, FL 33199, USA

³ USGS Pacific Coastal and Marine Science Center, 400 Natural Bridges Dr., Santa Cruz, CA 95060, USA

⁴ Department of Biological and Marine Sciences, Jacksonville University, MSRI Office 258, 2800 University Blvd, North Jacksonville, FL 32211, USA

Keywords Burrow flushing · Radon-222 (^{222}Rn) · Radium isotopes · Coastal groundwater discharge

Introduction

Like most coastal environments, fringe mangrove forests are dynamic and reflect a delicate balance between terrestrial and marine forcings. These coastal ecosystems are particularly dependent on sea level variations to maintain suitable habitat. Tidal fluctuations act to replenish nutrients, deliver sediment, and flush away excessive salts around the base of mangroves

(Boto and Bunt 1981). Of equal importance, these sea level changes redistribute other constituents (e.g., carbon) from the terrestrial and adjacent estuarine or marine environments (Troxler et al. 2015). The carbon budget of mangrove environments is dynamic and complex. Studies have shown that these systems may be globally important as both carbon sinks (Dittmar and Lara 2001; Breithaupt et al. 2012) as well as carbon sources to the coastal ocean (Dittmar et al. 2006). Sediment accumulation, carbon remineralization, and surface runoff are major factors affecting the long-term burial of carbon in these coastal ecosystems; however, recent studies have also shown that sustained groundwater discharge or benthic fluid exchange may be an important process influencing carbon transport and transformation in these estuarine systems (Maher et al. 2013).

Groundwater discharge to the coast incorporates a number of physical processes, fluid sources, and fluid transport pathways (Swarzenski 2007). To better understand material fluxes and exchange among various environments requires separation of processes (pumping, convection, or gravity driven flows) and the source water (marine or terrestrial) (Martin et al. 2007; Roy et al. 2010). Potential sources of groundwater to coastal systems generally fall into two categories: terrestrial, meteoric-derived fresh groundwater, and marine groundwater. The terrestrial or fresh submarine groundwater is driven by gravity flow to the coastal zone from upland, terrestrial areas that are most often recharged by rainfall (Younger 1996; Michael et al. 2005). The marine groundwater can range in salinity from brackish to hypersaline and originates as marine surface water that intrudes into the coastal aquifer (Badon-Ghyben 1889). The marine groundwater becomes chemically altered while in the aquifer owing to a number of processes including mixing with the fresh groundwater, water-rock interactions and redox processes (Moore 1999). The altered marine groundwater is then discharged to a surface water body (Cooper 1959). Both the marine and fresh groundwaters mix in the subsurface along a dispersive mixing zone or subterranean estuary (Moore 1999). Biogeochemical transformations that may affect nutrients, trace elements, and carbon take place in the subterranean estuarine part of the coastal aquifer and depend largely upon the contrast in chemical compositions between the two water sources but also the physical processes governing flow and residence time in an aquifer (Anderson et al. 2005; Kim and Swarzenski 2010). Subterranean estuaries can occur at a variety of spatial scales and are linked to the hydraulic gradients in the coastal aquifer on the terrestrial side and sea level variations on the marine side (Michael et al. 2005; Robinson et al. 2007; Santos et al. 2012).

In studies of submarine groundwater, discharge rates obtained by different measurement techniques can vary by an order of magnitude or more. This has been especially true for discharge rates derived from hydrological

budgets versus from radiochemical budgets (Burnett et al. 2006), as the two often reflect different source water and processes. In the case of the hydrologic budget, groundwater discharge is linked solely to a meteoric water source, while the geochemical budgets incorporate multiple water sources and processes. While terrestrial groundwater is the only source of allochthonous or new water into the systems, marine groundwater can have a significant influence on the biogeochemical cycling in the coastal zone as it acts on a number of time scales (seconds to years) (Santos et al. 2012). For example, bioirrigation and burrow flushing can be significant mechanisms for nutrient exchange and mass transfer in both subtidal and intertidal ecosystems (Berner 1980; Meile and Van Cappellen 2003). In subtidal environments, benthic fauna actively flush water into and out of burrows to maintain oxic conditions (Koretsky et al. 2002), while in intertidal regions, pressure change associated with tides can result in gradients that passively force water through burrows (i.e., tidal pumping) (Stieglitz et al. 2000). Based on temporally discrete sampling, Stieglitz et al. (2013) inferred from water column radon and radium budgets that tidal flushing of crab burrows (e.g., *Sesarma messa*, *Alpheus cf macklay*, and *Uca* spp.) had a significant influence on material export from mangrove forest to the adjacent estuary in Australia. Gleeson et al. (2013) and Maher et al. (2013) demonstrated the importance of quantifying material exchange over an entire tidal cycle. The importance of these interactive biological (burrowing) and physical processes (tidal variation and meteoric water inputs) becomes extremely important in low gradient systems such as wetlands and estuarine environments.

Identifying and quantifying the governing hydrologic and oceanic processes are critical for evaluating the role groundwater has on material cycling. For the low-gradient Florida Coastal Everglades (FCE), the discharge of meteoric and marine groundwater is closely tied to the surface water system (Price et al. 2003). Surface water flow in the region is seasonally controlled by rainfall. Annual precipitation averages 1320 mm and is distributed unequally during the wet season (~80 % between June and November) and dry season (20 % between December and May) (Duever et al. 1994). To identify and quantify contributions of groundwater to the Shark River Slough (SRS) in the Florida Coastal Everglades (FL, USA), we present geochemical data collected during both wet and dry seasons. The purpose of this paper is to identify and quantify in this setting yet unidentified pathways of groundwater input to SRS using a suite of radon and radium isotopes. From a systematic evaluation of ^{222}Rn budgets, tidal pumping and exchange within the mangrove forest contributes significantly to overall water budgets. Quantifying meteoric groundwater discharge by radioisotopes requires an accounting for the variance in export from the mangroves.

Study Area

The FCE are located in south-southwest peninsular Florida (Fig. 1a). Surface water export from the Everglades National Park (ENP) occurs through two primary riverine distributary systems: SRS which flows to the Gulf of Mexico and Taylor Slough (TS) that flows into northern Florida Bay. The SRS estuary (SRSE) is the lower estuarine portion of the SRS and is comprised of a number of different tidal distributaries—including the Shark, the Harney, Broad, and Lostman Rivers—that all empty into eastern Gulf of Mexico (Fig. 1a). The SRSE is tidally driven with a mean tidal range of 2.3 m. Overall, the climate of southwest Florida is defined by distinct wet and dry seasons. During our field investigations in the dry season (30 March to 3 April 2009), the 2-month and 2-week precipitation prior to sampling was 5.5 cm and 2.5 mm. Comparatively, the two wet season (11–16 September 2010 and 16–19 November 2010) sampling trips had 2-month/2-week precipitation totals of 389.4/145.3 mm and 119.4/66.5 mm, respectively (Elec. Supp. Material A1).

The ecological structure of the SRSE is characterized as a tidal, oligohaline mangrove ecotone. The modern mangrove forests are accumulating peat on top of previously accumulated fresh to brackish wetland environments (Wingard et al. 2006). Peat thickness shows a natural transgressive nature with the thickest deposits (~6 m) occurring near the mouth of the river and thins upstream (to the northeast) to less than a meter near Rookery Branch (RB on Fig. 1b; Gordon Anderson, personal communication). The peat overlies the Biscayne Aquifer, a carbonate aquifer comprised of the Miami Limestone, Fort Thompson, and Key Largo formations. In the vicinity of SRS, the Miami Limestone is the most prevalent (Parker et al. 1955).

Our study was conducted along the SRSE between RB and the Gulf of Mexico with moorings at FCE—Long-Term Ecological Research (FCE-LTER) monitoring station SRS-6 (25.36462994° N, 81.07794623° W) (Fig. 1b, c). The site is located approximately 3.5 km inland of the Gulf of Mexico along one of the main distributary channels that merge upstream with the Shark River. Tidal harmonics for the entire

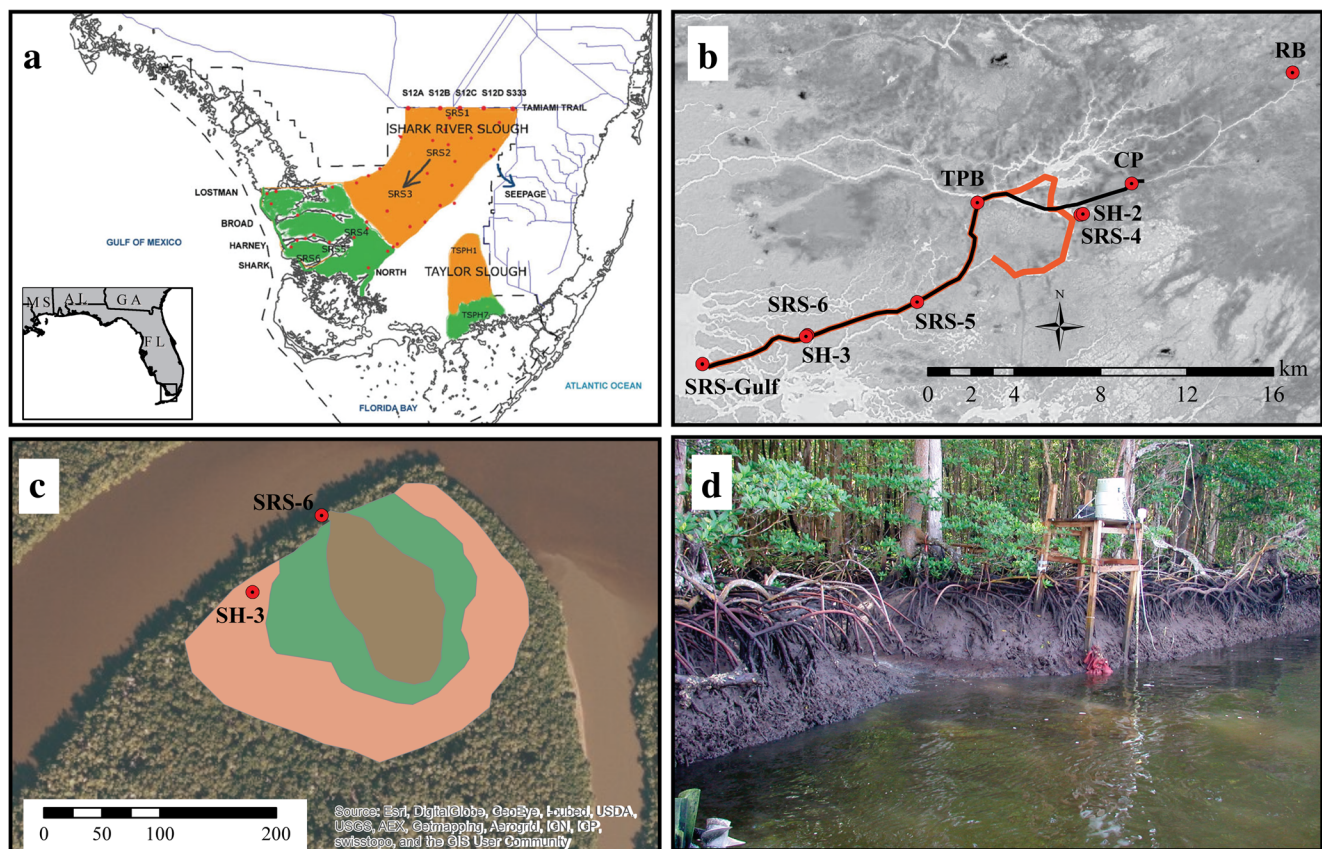


Fig. 1 a Map of the Florida Coastal Everglades—Long-Term Ecosystem Research showing the Shark River Slough and Shark River Slough estuary (green) along with the various surface collection sites. b A map showing the ^{222}Rn survey tracks overlain on a Landsat (USGS) mosaic of the Shark River Slough estuary. c Location of SRS-6 and nearby SH-3 along the Shark River Slough estuary with the different potential tidal flooding areas. The brown polygon shows the 10,000 m² reported as the

primary drainage area for SRS-6. The green and pink were extracted from historical aerial imagery during high water events (e.g., after Hurricane Wilma). The areal extent of the green and pink are 25,000 and 100,000 m², respectively. d A photograph taken up-stream of the tidal creek that drains the 10,000 m² mangrove forest around SRS-6. The abundant crab burrow hole is evident in the creek and river banks (color figure online)

slough and the site are semi-diurnal with a range that averages 1 m. Tidal wave propagation through the SRSE is approximately 5.8 cm s^{-1} based on water levels measured during November 2010 at gages distributed along Shark River (Elec. Supp. Material A2). The wave is dampened significantly up the estuary with an amplitude reduction of 60 %. The time series mooring for site SRS-6 is positioned next to a small tidal creek that drains approximately $10,000 \text{ m}^2$ of mangrove forest (FCE-LTER website, accessed 19 August 2014) (Fig. 1c, d). An assessment of historical imagery from the last 20 years showed that the drainage area may be as much as 25,000 to $100,000 \text{ m}^2$ during large storm tides (Fig. 1c), incorporating much of the northern portion of the mangrove forest island (Wdowinski et al. 2013).

Methods

Field Sampling

Temporal variations in surface water radon and radon-derived-groundwater discharge rates were examined at SRS-6 by conducting field investigations during wet and dry seasons (Fig. 1c, d). During each sampling trip, continuous radon-222 (^{222}Rn) was monitored at one mooring station while surface water ^{222}Rn was mapped throughout the estuary (Figs. 1b and 2). Additional surface water and groundwater samples were collected from discrete locations throughout the tidal basin to characterize potential fluid sources using $^{223,224,226}\text{Ra}$. For reporting convenience, ^{222}Rn data are presented as dpm L^{-1} , while radium isotopes are reported as dpm m^{-3} . The scaling factor between the two is 1000 (i.e., $\text{dpm L}^{-1} \times 1000 = \text{dpm m}^{-3}$).

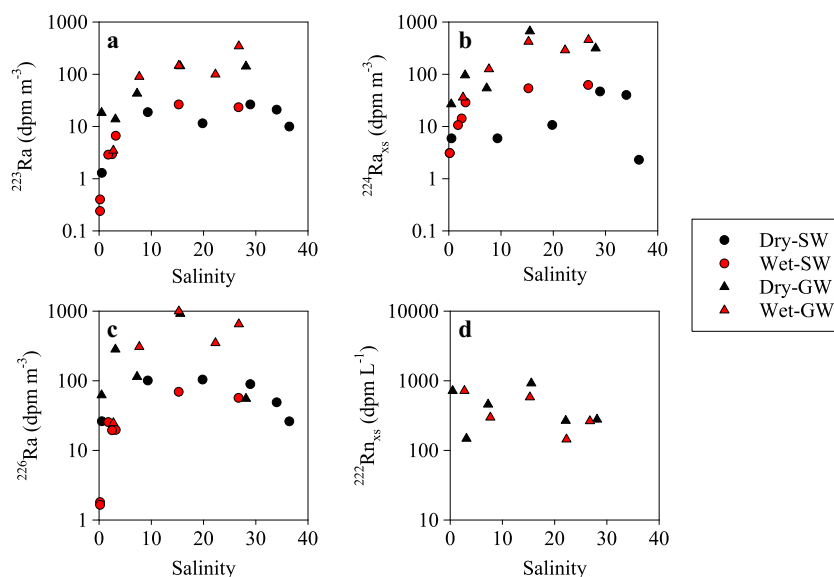
Time Series Mooring

During each investigation, water column radon was measured continuously (0.5-h intervals) over a 2- to 3-day period. Continuous radon monitoring followed the methodology described in Burnett et al. (2001). Briefly, surface water was continuously pumped and sprayed into an air-water exchanger where radon was degassed from the water into the headspace of the exchanger. The extracted radon was then drawn from the exchanger into a radon-in-air detector (RAD7, DurrIDGE). Temperature and salinity in the exchanger were also continuously monitored to correct for thermal and “salt” effects on radon partition between water and air as described by Schubert et al. (2012). Ambient radon-in-air was also monitored at one site during each investigation. Wind speed data were obtained from an eddy flux tower located at SRS-6; wind fields were considered uniform throughout the study area and applied to all sampling locations. Surface water temperature, conductivity, and pressure were also continuously monitored at the intake of the submersible pump.

Discrete Sampling

Groundwater and surface water were sampled at several sites along Shark River (Fig. 1b). “Deep” groundwater (defined operationally as being greater than 100 cm below the land surface, cmbs) was collected from five preexisting wells distributed across the entire estuarine gradient (RB, CP, SH-2, TPB, SH-3); surface water was also collected from the river channel proximal to each well, prior to sampling the well. Approximately three well volumes were purged from each well prior to sampling. The water quality parameters temperature, conductivity, dissolved oxygen, ORP, and pH were

Fig. 2 The activities of ^{223}Ra , $^{224}\text{Ra}_{\text{xs}}$, ^{226}Ra , and $^{222}\text{Rn}_{\text{xs}}$ collected from surface water (circles) and groundwater (triangles) during the dry (black) and wet (red) seasons presented as a function of measured salinity (color figure online)



monitored until stable readings were obtained while the wells were being purged. The same stabilization criteria were used for surface waters as well. Pore water was collected between slack water low tide and the first hour of flood tide at SRS-6 during the dry and wet seasons using shallow stainless-steel push-point samplers (M.H.E. Products) and a peristaltic pump. Total pore water volume extracted from each sampling depth was kept to a maximum of 180 mL (Smith and Swarzenski 2012). Pore waters were analyzed for salinity only in the field using a calibrated field refractometer. Radon-222 in both groundwater and pore water was measured using a direct count method via liquid scintillation (Smith et al. 2008, Smith and Swarzenski 2012). Efficiency and MDA for all runs associated with this study averaged 2.42 ± 0.08 cpm dpm⁻¹ and 22.8 ± 9.6 dpm L⁻¹, respectively.

Dissolved radium was extracted from groundwater and surface water (30–50 L) at a flow rate of 1 L min⁻¹ onto preweighed manganese fiber (Mn fiber) following Moore and Reid (1973). Total ^{223,224}Ra and supported ²²⁴Ra absorbed on the Mn fiber were measured using a Radium Delayed Coincidence Counter (RaDeCC, Scientific Instrument) designed by Moore and Arnold (1996). While individual system efficiencies were applied to measurements, the temporal stability and across system comparisons were high as efficiencies for ²¹⁹Rn, ²²⁰Rn, and total averaged across all four units and over the 2-year study were 0.30 ± 0.07 , 0.41 ± 0.07 , and 1.08 ± 0.09 cpm dpm⁻¹, respectively. Radium-226 on the Mn fiber was also quantified in a similar way; ²²²Rn in secular equilibrium with ²²⁶Ra was circulated through a close-loop interfaced with a radon-in-air monitoring device (RAD7, DurrIDGE) (Kim et al. 2001; Dulaiova et al. 2005; Peterson et al. 2009). Average efficiency for the procedure used over the 2-year period was 0.13 ± 0.03 cpm dpm⁻¹, and average MDA was 0.9 dpm L⁻¹. Excess ²²²Rn (²²²Rn_{xs}) was computed as the difference between measured total ²²²Rn and ²²⁶Ra (i.e., supported ²²⁶Ra). Uncertainty in ²²²Rn_{xs} was propagated using standard procedures from measured total and supported ²²²Rn.

Surface Water Surveys

Surface water ²²²Rn was measured continuously in March/April 2009 and November 2010. During the surveys, geographic position (WGS84) and water depth were recorded continuously at 5-s intervals shipboard on a Garmin Echomap 50s (Garmin, Ltd.). While underway, surface water was continuously pumped (2 to 5 L min⁻¹) from a side mount lowered to 0.5 m below the water surface that flowed to an air-water equilibration chamber. Radon was separated from the water into the headspace of the chamber. Using four commercially available, radon-in-air detection devices with internal air pumps (Rad7, DurrIDGE, Inc.), ²²²Rn in the air phase was circulated and analyzed via its short-lived decay product polonium-218. Count integration time for both trips was 10 min.

Temperature and salinity were continuously monitored in the exchanger to accurately convert in-air concentrations to in-water concentrations. Based on ambient air count rates measured before, during, and after the surveys, the effective minimum detectable activity (MDA) in the system was 0.24 ± 0.05 dpm L⁻¹ ($n=4$). All errors are reported to one standard deviation unless otherwise noted. In addition to ²²²Rn, salinity and temperature were measured continuously using a flow-through conductivity and temperature probe system (YSI-556). All data were post-processed with GPS and integrated in spatial data layers using ArcGIS version 9.3 (ESRI, Inc.)

Modeling Benthic Fluxes

We compare two separate ²²²Rn mass balance approaches to evaluate benthic fluid contributions from mangrove forest to the creek and subsequently Shark River. The first model uses the tidal prism and concentration ratio to calculate a volume of water discharged from the mangrove forest floor (Peterson et al. 2009). This box model approach can be done for specific times or over a more complete tidal cycle (i.e., tidal prism, V_{tp} , m³). Assuming complete tidal exchange, the volume ($V_{mangrove}$) of water exchanged with the mangrove forest follows the computation of Crusius et al. (2005) and Peterson et al. (2009):

$$V_{mangrove} = \frac{(\bar{C}_{ebb} - \bar{C}_{flood})}{C_{mangrove}} V_{tp} \quad (1)$$

where \bar{C}_{ebb} , \bar{C}_{flood} are the mean ebb and flood concentrations of ²²²Rn (dpm L⁻¹), respectively, and $C_{mangrove}$ is the mangrove forest pore water end-member. Such approach is relatively conservative as it neglects additional loss terms of ²²²Rn within the mass balance. Conversely, it also assumes that the groundwater dominates neglecting diffusive inputs.

A similar approach can be used with the time series measurements of ²²²Rn activity of water entering and exiting the tidal creek to evaluate net fluxes following the procedure similar to Burnett et al. (2007) and Stieglitz et al. (2013). The model tracks the change in excess inventory (ΔI_{xs} ; dpm m⁻²) over time (Δt) following corrections for radioactive decay, tidal dilution, and radioactive ingrowth from dissolved ²²⁶Ra (Burnett et al. 2007). While atmospheric loss and mixing are other potential loss terms, both are ignored for this setting. Evasion is considered negligible as the dense vegetation (Fig. 1d) reduces wind shear beneath the forest canopy, and the flow is assumed to be laminar during flood and ebb tides. Mixing is assumed to be unimportant as we expect most of the water entering the forest is also leaving. Thus, the net change in inventory over the course of a tidal period (T , h) provides an estimate of a ²²²Rn tidal flux ($f_{net|tide}$, dpm m⁻² T⁻¹) from the mangrove forest.

$$\left. \frac{\Delta I_{xs}}{\Delta t} \right|_T = f_{net/tide} \quad (2a)$$

The tidal period may vary depending on the character of the tide (i.e., diurnal, semi-diurnal, or mixed semi-diurnal) influencing a representative period for integration.

Assuming a closed-tidal system, only diffusion and advection contribute to the net tidal flux (i.e., the integrated inventory observed during flooding versus the integrated inventory observed during ebb). The diffusive flux (f_{diff}) was estimated using the approach presented by Martens et al. (1980):

$$f_{diff} = (C_{mangrove} - \overline{C_{flood}}) \sqrt{\lambda D_s} \quad (2b)$$

where D_s is the temperature- and tortuosity-corrected molecular diffusion coefficient ($\text{m}^2 \text{day}^{-1}$) and λ is the decay coefficient (0.181day^{-1}). The resulting relationship for the tidal volume of fluid originating from the mangrove forest is

$$V_{mangrove} = \frac{(f_{net/tide} - f_{diff})}{C_{mangrove}} A_{high} T \quad (2c)$$

Dividing the linear flux by a representative ^{222}Rn activity for mangrove forest results in a linear flux of water (i.e., flux over a tidal period) from the mangrove forest that can be extrapolated over the entire tidal period (T) and the forest floor (A_{high} , m^2) at high tide.

Results

Radioisotopes and Salinity Across SRSE

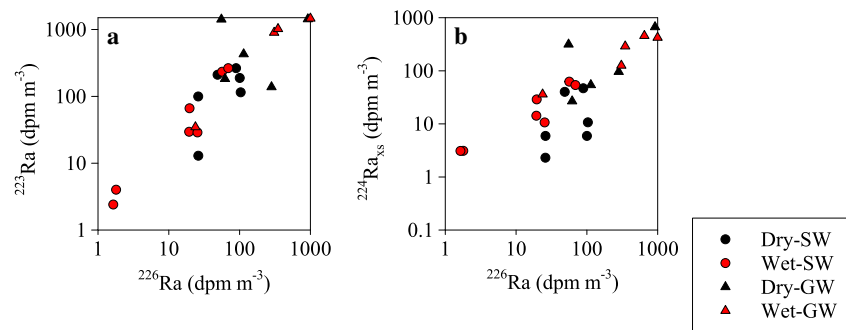
The groundwater salinity remained fairly constant for both the wet and dry season sampling (Table 1). A regression analysis between wet season salinity and dry season salinity at each wells resulted in a slope 0.976 ($r^2=0.965$). All the radium isotopes in groundwater increased through the low brackish salinity range and were relatively constant at salinities greater than 10 (Fig. 2a–c). Excluding two extreme values (Table 1), the ratio of $^{224}\text{Ra}/^{226}\text{Ra}$ was quite similar for both the dry and wet season (0.49 ± 0.14 and 0.59 ± 0.18 , respectively) as was $^{223}\text{Ra}/^{226}\text{Ra}$ (0.22 ± 0.13 and 0.32 ± 0.14 , respectively) (Fig. 3). Excess ^{222}Rn in groundwater did not consistently covary with salinity in space or time (Fig. 2d).

Table 1 Field parameters, radionuclide activities, and activity ratios from discrete samples of groundwater and pore water

Season	Site name	Date sampled	Depth (m)	Temp (°C)	Salinity	$^{222}\text{Rn}_{xs}$ (dpm L^{-1})	^{223}Ra (dpm m^{-3})	$^{224}\text{Ra}_{xs}$ (dpm m^{-3})	^{226}Ra (dpm m^{-3})	$^{224}\text{Ra}/^{226}\text{Ra}$
Dry										
	SH-3	March 31, 2009	7.33	24.6	28.1	277 ± 17	141.7 ± 2.4	314.2 ± 4.9	55 ± 7	5.69
	SH-2	April 1, 2009	3.76	21.8	7.3	456 ± 43	42.9 ± 1.2	54.0 ± 1.2	114 ± 9	0.47
	SH-1	April 3, 2009	3.26	23.7	0.5	715 ± 88	18.3 ± 0.8	26.7 ± 1.1	62 ± 5	0.43
	CP-GW	March 31, 2009	15.5	24.5	15.5	919 ± 59	143.1 ± 2.3	667.3 ± 6.8	918 ± 55	0.73
	RB-1A-GW	April 1, 2009	6.70	24.5	3.1	147 ± 7	13.8 ± 0.8	95.9 ± 2.3	282 ± 53	0.34
	TP-GW	April 2, 2009	19.8	24.6	22.1	267 ± 51	nd	nd	nd	nd
	SH-3pw-30 cm	March 31, 2009	0.30	nd	33.8	96 ± 18	nd	nd	nd	nd
	SH-3pw-65 cm	March 31, 2009	0.60	nd	33.7	95 ± 15	nd	nd	nd	nd
Wet										
	SH-3	September 13, 2010	7.33	28.1	26.8	263 ± 14	345.2 ± 11.2	456.0 ± 12.0	650 ± 67	0.70
	SH-2	September 13, 2010	3.76	26.6	7.7	297 ± 6	90.0 ± 5.3	125.8 ± 5.6	308 ± 39	0.41
	CP-GW	September 13, 2010	15.5	26.1	15.3	579 ± 12	146.2 ± 4.2	422.7 ± 6.5	1000 ± 74	0.42
	RB-1A-GW	September 13, 2010	6.70	24.7	2.7	717 ± 40	3.5 ± 0.4	36.1 ± 1.4	25 ± 4	1.46
	TP-GW	September 14, 2010	19.8	27.2	22.3	144 ± 18	99.6 ± 8.8	289.8 ± 13.8	350 ± 40	0.83
	SH-3-PW	November 19, 2010	0.1	nd	nd	35 ± 23	nd	nd	nd	nd
	SH-3-PW	November 19, 2010	0.2	nd	nd	61 ± 11	nd	nd	nd	nd
	H-3-PW	November 19, 2010	0.3	nd	nd	105 ± 7	nd	nd	nd	nd
	SH-3-PW	November 19, 2010	0.4	nd	nd	89 ± 9	nd	nd	nd	nd
	SH-3-PW	November 19, 2010	0.5	nd	nd	60 ± 9	nd	nd	nd	nd
	SH-3-PW	November 19, 2010	0.75	nd	nd	172 ± 5	nd	nd	nd	nd

nd not determined

Fig. 3 The activities of ^{223}Ra (a) and $^{224}\text{Ra}_{\text{xs}}$ (b) collected from surface water (circles) and groundwater (triangles) during the dry (black) and wet (red) seasons presented as a function of the longer lived ^{226}Ra



Groundwater ^{222}Rn activities ranged from 280 to 920 and 140 to 720 dpm L^{-1} for the dry and wet seasons, respectively, with an overall mean of $410 \pm 240 \text{ dpm L}^{-1}$ ($n=10$). Average radon activities in pore water from the upper 60 cmbls, which encompasses much of the burrowing zone, were not statistically different between the dry ($96 \pm 1 \text{ dpm L}^{-1}$) and wet ($70 \pm 24 \text{ dpm L}^{-1}$) seasons.

Discrete surface water samples collected across the estuary at low tide reiterate the influence of seasonal precipitation on the salinity structure (Table 2) and mixing within SRSE. Low-tide salinity values from the discrete sites were 0.5 to 36.4 for the dry season and 0.5 to 26.7 for the wet season. Radium isotopes also varied between the two seasons; however, all three radium isotopes demonstrated an increase in activity in mid-salinity ranges (Fig. 2a–c). The activity of ^{226}Ra showed a qualitative enrichment with respect to salinity for both the dry and wet season, with maxima

($\sim 1000 \text{ dpm m}^{-3}$) occurring around a salinity of 22.0 (Fig. 2c). However, the maxima for radium isotopes were observed further downstream during the wet season (SRS-Gulf) than during the dry season (Tarpon Bay) due to the generally fresher conditions in the former. The activities of ^{223}Ra and ^{224}Ra had very well defined maxima in the dry season (Fig. 2b, c). During the dry season only, the ratio $^{224}\text{Ra}/^{226}\text{Ra}$ (0.67 ± 0.15 , $n=2$) was distinct in this zone of elevated radium relative to other portions of the estuary (0.08 ± 0.01 , $n=3$) and quite similar to the dry season groundwater activity ratio (0.49 ± 0.14). Also, $^{224}\text{Ra}/^{226}\text{Ra}$ for the two seasons is distinct. In the dry season, the ratio is between 0.1 and 0.8 and similar to that observed in the groundwater (~ 0.4), while during the wet season, it generally exceeds 1. The radium isotope distribution and ratio data suggest additional sources of all isotopes to the estuary.

During the surface water surveys, the activity of ^{222}Rn varied between the dry and wet season; however,

Table 2 Field parameters, radionuclide activities, and activity ratios from discrete samples of surface water samples collected at low tide

Season	Site name	Date sampled	Latitude	Longitude	Depth (m)	Temp (°C)	Salinity	^{223}Ra (dpm m^{-3})	$^{224}\text{Raxs}$ (dpm m^{-3})	^{226}Ra (dpm m^{-3})	$^{224}\text{Ra}/^{226}\text{Ra}$
Dry	SRS-Gulf	March 31, 2009	25.3536	-81.1216	0.50	24.45	36.4	9.9 ± 0.6	2.3 ± 0.1	26.0 ± 2.1	0.09
	SRS-6	March 31, 2009	25.3646	-81.0779	0.50	25.39	34.0	20.9 ± 0.8	40.0 ± 1.3	48.8 ± 2.4	0.82
	SRS-5	March 31, 2009	25.3771	-81.0323	0.50	25.86	29.0	26.3 ± 0.9	46.6 ± 1.2	89.1 ± 7.1	0.52
	SRS-4	April 1, 2009	25.4098	-80.9643	0.50	28.09	19.8	11.5 ± 0.7	10.7 ± 1.2	103.5 ± 11.2	0.10
	CP-SW	March 31, 2009	25.4215	-80.9430	0.50	26.83	93	18.7 ± 0.8	5.9 ± 0.2	100.3 ± 8.0	0.06
	RB-1A-SW	April 1, 2009	25.4633	-80.8760	0.50	23.87	0.5	1.3 ± 0.2	5.9 ± 0.6	26.1 ± 2.1	0.23
	TP-SW	April 1, 2009	25.4144	-81.0071	0.50	26.98	21.4	nd	nd	nd	nd
Wet	SRS-Gulf	September 14, 2010	25.3536	-81.1216	0.50	26.7	26.7	23.3 ± 2.3	62.2 ± 3.8	56.5 ± 11.2	1.10
	SRS-6	September 14, 2010	25.3646	-81.0779	0.50	29.52	15.3	26.3 ± 2.6	53.7 ± 3.2	69.1 ± 12.5	0.78
	SRS-5	September 13, 2010	25.3771	-81.0323	0.50	30.21	3.2	6.6 ± 0.4	28.8 ± 1.0	19.6 ± 7.1	1.47
	SRS-4	September 12, 2010	25.4098	-80.9643	0.50	30.27	2.5	2.9 ± 0.2	14.2 ± 0.5	19.4 ± 9.5	0.73
	CP-SW	September 12, 2010	25.4215	-80.9430	0.50	30.17	0.2	0.4 ± 0.1	3.1 ± 0.2	1.8 ± 8.0	1.72
	RB-1A-SW	September 13, 2010	25.4633	-80.8760	0.50	28.9	0.2	0.2 ± 0.1	3.1 ± 0.4	1.6 ± 2.0	1.88
	TP-SW	September 12, 2010	25.4144	-81.0071	0.50	30.36	1.8	2.9 ± 0.2	10.6 ± 0.4	25.4 ± 6.7	0.42

nd not determined

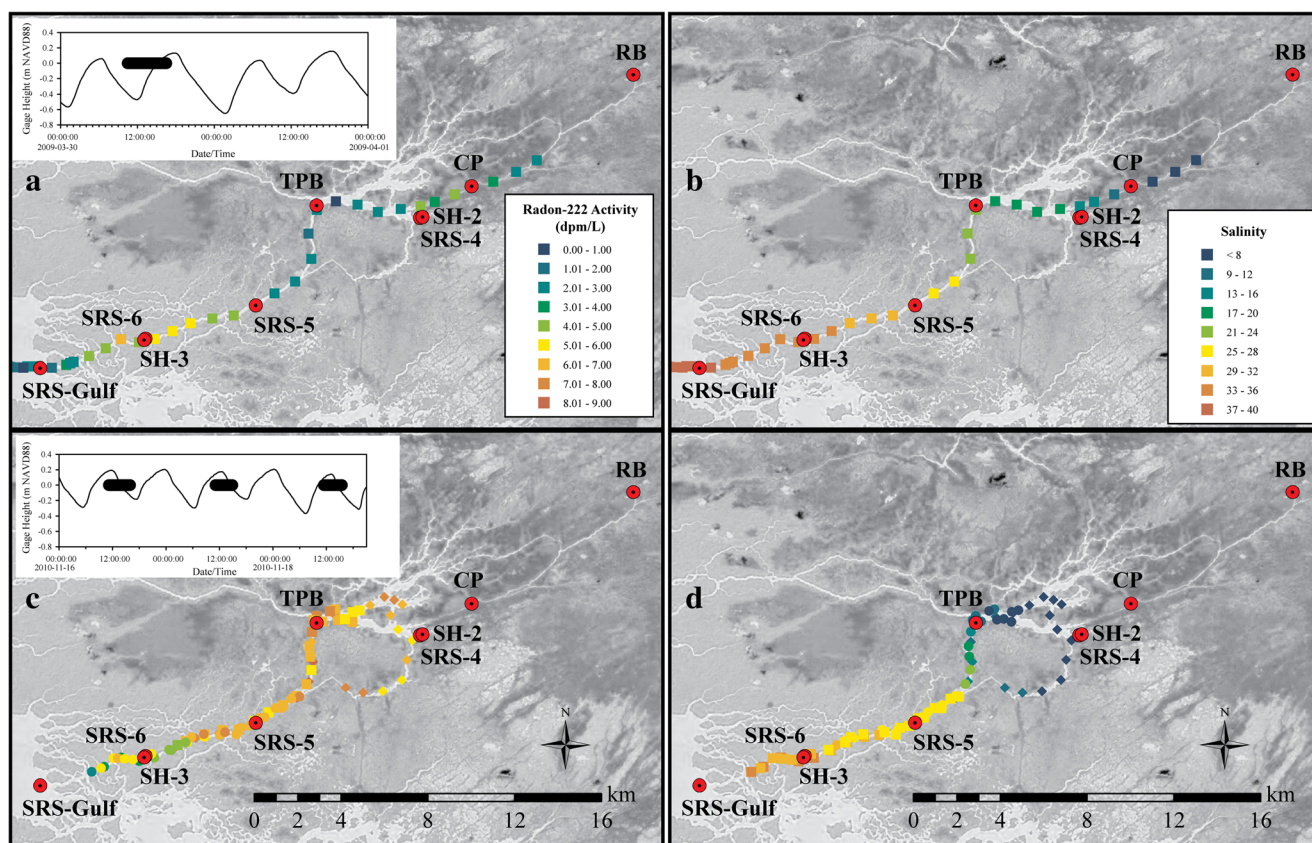


Fig. 4 The distribution of ^{222}Rn (a, c) and salinity (b, d) measured during the dry season (top row; a, b) and the wet season (bottom row; c, d)

salinity distribution was relatively similar for the two surveys (Fig. 4). During the dry season, data were collected at low-to-flood tide. For the region between Tarpon Bay and SRS-6 (region of overlap for both surveys), surface water ^{222}Rn varied between 0.9 and 6.1 dpm L^{-1} but was skewed toward the lower end with a mean of $3.8 \pm 1.4 \text{ dpm L}^{-1}$ ($n=18$). Salinity ranged between 8.1 and 32.9 and a mean of 21.2 for the same region. The range is higher than the discrete samples as surveying was limited to areas downstream of and including Tarpon Bay. During the wet season, data were collected during high-to-ebb tides (Fig. 4b). The magnitude of ^{222}Rn in the surface water during the wet season was notably higher ($6.6 \pm 1.0 \text{ dpm L}^{-1}$, $n=57$) than the dry season ($3.8 \pm 1.4 \text{ dpm L}^{-1}$, $n=18$). Wet season salinity had a range of 2.5 to 25.4 and a mean of 15.6, which based on mean and range were suppressed relative to the dry season. Using SRS-5 as a point of reference, salinity at this site was 27.2 and 24.9 during the dry and wet surveys, respectively. Overall, there is notable contrast between the wet and dry season mapping of ^{222}Rn ; however, the areas north of Tarpon Bay and adjacent to SRS-6 showed relatively higher ^{222}Rn activity during both surveys than other portions of the SRSE.

Temporal Variation in Salinity and Radon

Salinity and ^{222}Rn activity varied with tidal stage (Figs. 5, 6, and 7). Connection between the creek mouth and the interior mangrove forest is visible (Figs. 5, 6, and 7). In both the dry and wet seasons, water levels in the mangrove forest return to baseline conditions during successive tides. An offset between maximum water level and salinity is on the order of 10–30 min and does not appear to vary with season. However, the average salinity and salinity variability differ significantly between the dry and the wet season. During the dry season, salinity of the water draining the mangrove forest averaged 33.0 and ranged 31.3 to 34.5. In contrast, surface water salinities in September and November 2010 were much lower with averages of 18.3 and 27.5, respectively. The range during the wet season was also much greater (salinity range of 9–10) than the dry season.

The activity of ^{222}Rn covaried with surface water levels but with a more pronounced lag than salinity and had characteristics linked to differences in the tidal harmonics (i.e., semi-diurnal vs. mixed semi-diurnal). Mean ^{222}Rn activities for the dry and wet seasons differed by 30 % (i.e., 12.9 and 9.3 dpm L^{-1} , respectively). The range in activity during the dry season relative to the mean (67 %) was notably

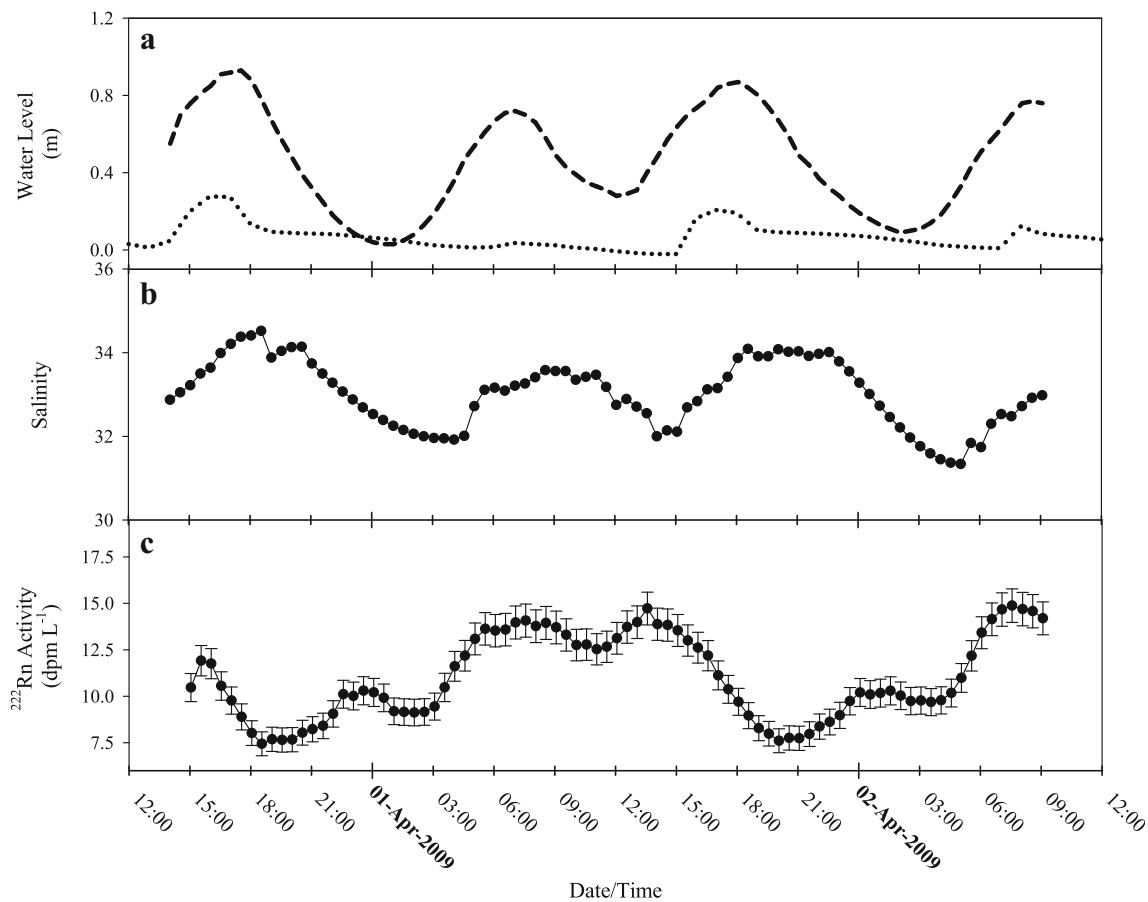


Fig. 5 Time series data of water levels (**a**), salinity (**b**), and ^{222}Rn activity (**c**) collected from the creek mouth during the dry season in March and April 2009. **a** Water level data for both the creek mouth (*dashed*) relative to the creek bottom and the mangrove forest (*dotted*) relative to the mangrove floor

higher than during the wet season (34 %) (Table 3). The tidal harmonics also influenced the surface water ^{222}Rn activity. During the dry season and the first wet season (September 2010) sampling, the tides were mixed semi-diurnal. Under this type of tide, ^{222}Rn activity only peaked once during a complete 24.83-h tidal cycle. In contrast, the November 2010 sampling occurred during a semi-diurnal tide and ^{222}Rn showed an identical but out-of-phase, semi-diurnal modulation.

Discussion

Tidal Pumping of the Mangrove Forest Peat

Stieglitz et al. (2013) noted that spatial scaling is important in assessing the overall impact of mangrove forests on local estuarine and coastal ocean material budgets; however, temporal variance (seasonal or daily) complicates any attempts at upscaling. The importance of temporally varying processes on surface water-groundwater exchange is well documented and has been shown to significantly impact material cycling in permeable systems (Robinson et al. 2007; Swarzenski et al.

2007; Smith et al. 2008; Roy et al. 2010; Santos et al. 2010). Recently, the impacts that macrofauna burrows have on facilitating fluid and material exchange in mangrove and marsh systems have been presented (Gleeson et al. 2013; Maher et al. 2013). The temporal variability of ^{222}Rn activities measured at SRSE highlight the significance of both the tidal and potential seasonal controls on exchange between creeks and the mangrove peat.

^{222}Rn inventories and fluxes corrected for simple dilution retain the tidal signature observed in the activity (Figs. 5, 6, and 7). This variability is the basis of the net flux approached utilized with Eq. 2. The cumulative net flux of ^{222}Rn for each sampling trip from the mangrove forest was assessed based on tide. The dry and first wet season samplings were integrated from slack low-low tide to slack low-low tide (Table 3). Depending on the asymmetry of the tide, the cumulative net fluxes ranged less than an order magnitude ($5.6\text{--}38 \times 10^6 \text{ dpm T}^{-1}$) for the three sampling trips (Table 3). In comparison, the contribution from diffusion alone was between 1 and 10 % (i.e., $7.1\text{--}7.3 \times 10^5 \text{ dpm T}^{-1}$) of the total flux.

Both the tidal prism and the tidal flux models provide comparable fluid fluxes. For the tidal prism approach,

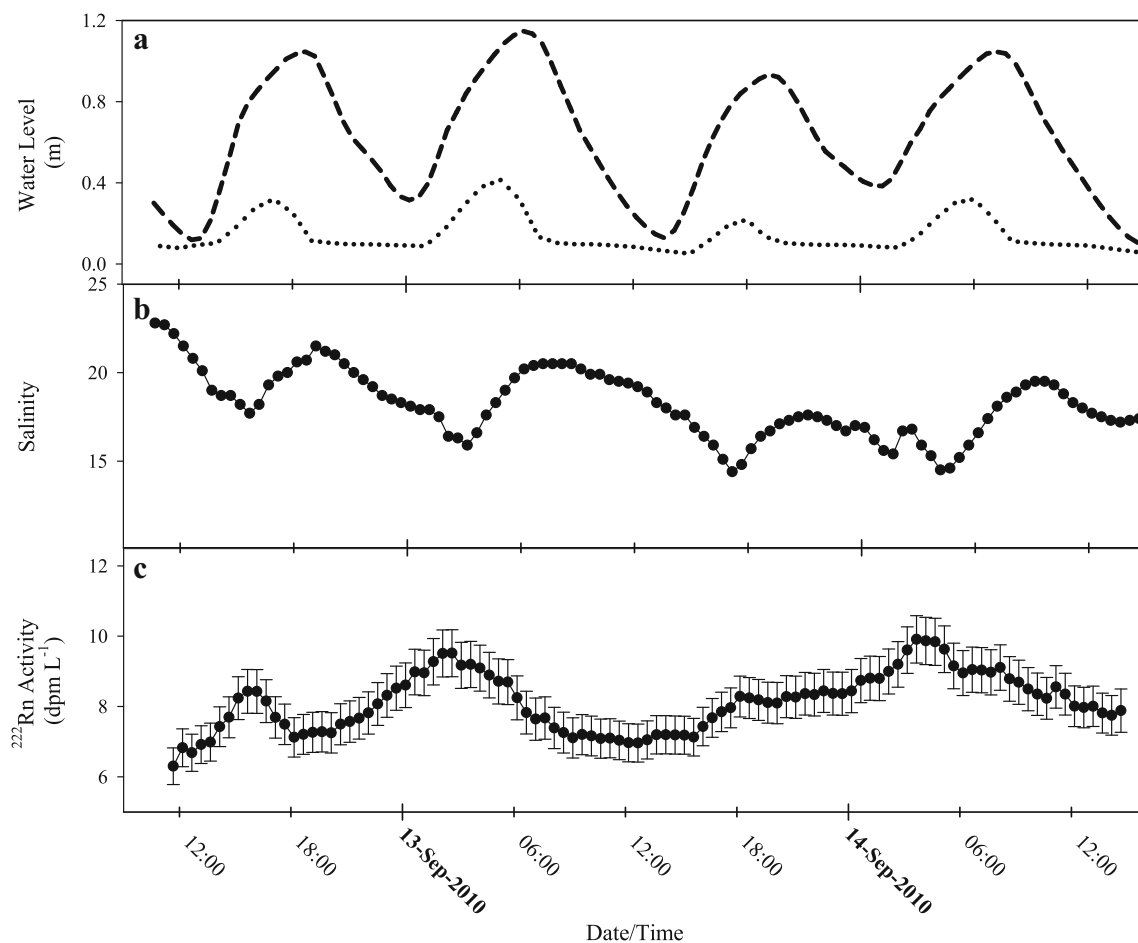


Fig. 6 Time series data of water levels (a), salinity (b), and ^{222}Rn activity (c) collected from the creek mouth during the wet season in September 2010. a Water level data for both the creek mouth (*dashed*) relative to the creek bottom and the mangrove forest (*dotted*) relative to the mangrove floor

Eq. 1 is not sensitive to the nature of the tide and can be used under the assumption of complete exchange of water over the course of a tidal period. Thus, each low-to-low tide period was used despite slight differences in the tidal amplitude (Table 3). Using Eq. 1 with mangrove end-member activities of 96 and 70 dpm L^{-1} for the dry and wet seasons, respectively, the range in discharge attributed to flushing of mangrove forest floor ranged between roughly 65 and 297 $\text{m}^3 \text{day}^{-1}$. Discharge rates in the dry season were two to three times higher than during the wet season. This was consistent with the larger gradient between the flood and ebb ^{222}Rn activity observed during the dry season. Similarly, the average of the two wet season flux estimates was within error of one another. Larger fluid fluxes ($\sim 30\%$) were observed during the lower low tide of the mixed semi-diurnal tide than during the higher low tide (Table 3). This may be due in part to slight variation in the flooded area during subsequent high tides. Based on water level data in from the mangrove forest (Figs. 5, 6, and 7), flooding depths and thus flooding extent were consistent for the April 2009,

September 2010, and the latter part of the November 2010 study periods. Assuming the linear relationship between areal extent of flooding and the radon/fluid flux in Eq. 2c holds, A_{high} would have to increase by 50% during the higher high tides observed during the first part of the November 2010 trip, making the percentages roughly offset. Discharge based on ^{222}Rn tidal fluxes had a similar range (68–374 $\text{m}^3 \text{day}^{-1}$) and seasonal characteristic as was observed using the tidal prism approach. Overall, the similarity between the fluid fluxes obtained by the two ^{222}Rn mass balance approaches suggest that benthic exchange dominates the temporal variability in the ^{222}Rn data over the time scale of the study. Also, quantitative and comparable estimates of groundwater discharge can be obtained using either technique.

The semi-diurnal variability in ^{222}Rn activity, salinity, and water level within the mangrove forest highlights the potential impact that contrasting tides (i.e., mixed semi-diurnal) can have on material and fluid exchange (e.g., Troxler et al. 2015). The variability in ^{222}Rn -based fluid fluxes between successive tides is low and within error.

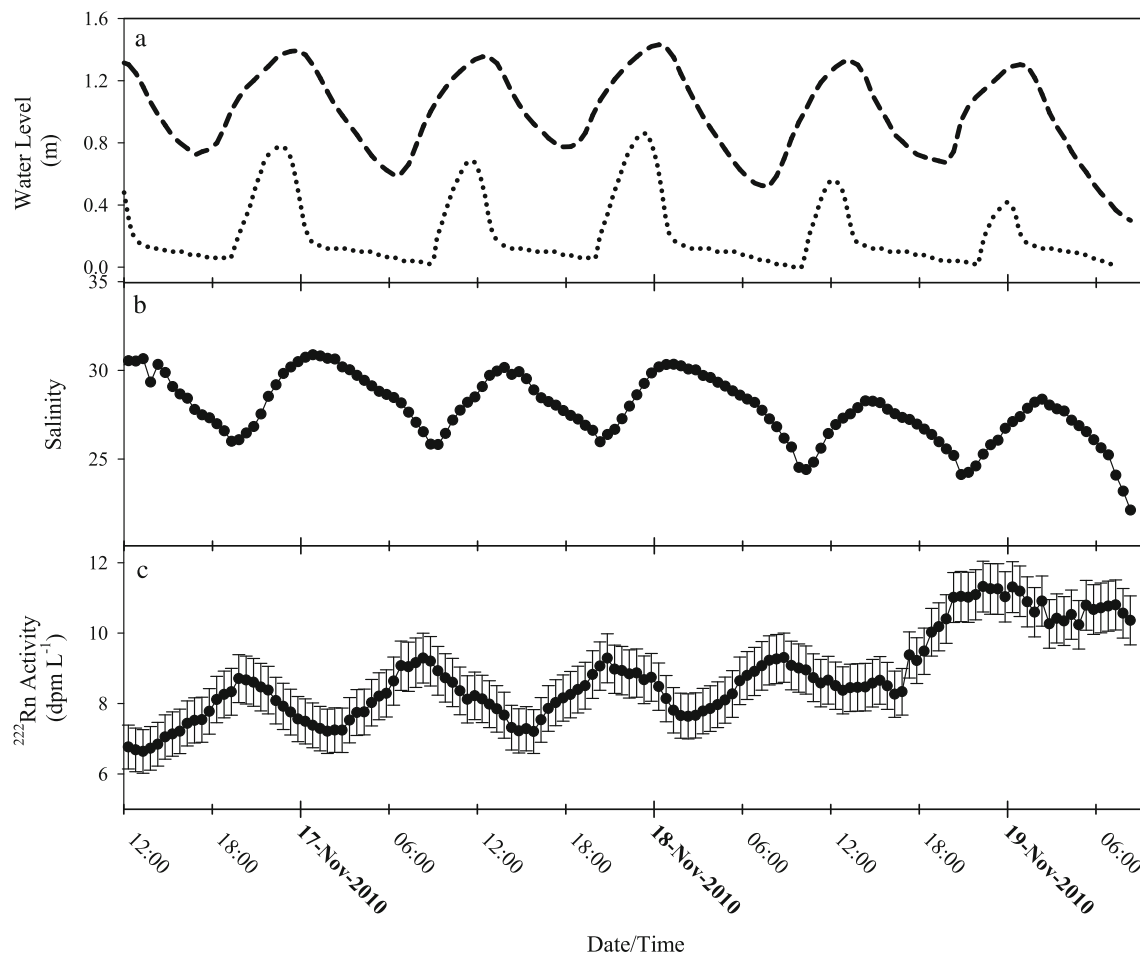


Fig. 7 Time series data of water levels (a), salinity (b), and ^{222}Rn activity (c) collected from the creek mouth during the wet season in November 2010. a Water level data for both the creek mouth (*dashed*) relative to the creek bottom and the mangrove forest (*dotted*) relative to the mangrove floor

However, the lagged response in salinity and ^{222}Rn activity provide clear evidence that the forest continues to drain as water levels in the creek mouth shift between slack and flood tides. During the higher low tide, a hysteresis effect results in an increase of residence time. On the successive lower low tide, water levels and radon indicate that there is more complete drainage. Our two approaches for examining fluid exchange does not directly account for this hysteresis and its mere observation warrants further investigation. While our methods do not account specifically for this hysteresis, assessing fluxes over the diurnal tidal cycle the fluid flux estimates are conservative.

Potential Controls on Seasonal Variability in the Mangrove Forest

Comparatively, the two wet season samplings have similar radon fluxes but differ significantly from the dry season. This seasonal variability may have implications for material export from the mangrove forest. Similar seasonal variations

have been reported in both mangrove and marsh settings. Gleeson et al. (2013) observed seasonal variability in radon fluxes in a mangrove system located in South Moreton Bay, Australia. In their study, higher fluxes occurred during the wet season (summer) as opposed to the dry season, which they attributed to enhanced biological activity. Our observations at SRSE indicate higher radon fluxes during the dry season over the wet season. The enhanced fluxes are due to the higher radon activities exiting the flooded swamp and associated steeper gradients in the dry season relative to the wet season. There is no ancillary data to suggest a difference in biological activity like that suggested in Australia. Thus, at SRSE, we suggest two possibilities to account for the seasonal variable radon fluxes: (1) there is an additional source of ^{222}Rn (e.g., deeper groundwater) during the dry season or (2) a variation in tidal flushing of the mangrove soil.

Discharge of deep groundwater from the Biscayne Aquifer has been recognized from chemical mass balance in the mangrove ecotone of the coastal Everglades (Price et al. 2003; Price et al. 2006). The higher radon fluxes could be related to seepage of groundwater from the underlying carbonate

Table 3 Radon-222 concentrations and fluxes used to evaluate fluid fluxes from the tidal prism model and the integrated net flux approach

Season	Date	Ebb $^{222}\text{Rnxs}$ (dpm L ⁻¹)	1σ	Tidal prism approach			Volumetric flux, $Q_{mangrove}$ (m ³ day ⁻¹)	Unc.	Net $^{222}\text{Rnxs}$ flux, $J_{mangrove}$ (dpm T ⁻¹)	Unc.	Net flux approach		
				Flood $^{222}\text{Rnxs}$ (dpm L ⁻¹)	1σ	Diffusive $^{222}\text{Rnxs}$ Flux, J_{diff} (dpm T ⁻¹)					Unc.	Volumetric Flux, $Q_{mangrove}$ (m ³ day ⁻¹)	Unc.
Dry	April 2009	14.1	0.9	9.1	0.7	307	63	3.78E+07	1.43E+07	7.07E+05	3.48E+04	413	156
Dry	April 2009	15.2	0.5	7.6	0.6	471	42						
Wet	September 2010	8.6	0.6	6.7	0.5	133	22	1.02E+07	7.14E+06	7.14E+05	2.01E+05	106	74
Wet	September 2010	9.5	0.6	7.0	0.5	178	29						
Wet	September 2010	8.8	0.6	7.1	0.5	117	19	9.75E+06	6.38E+06	7.14E+05	2.01E+05	101	66
Wet	September 2010	9.9	0.6	7.7	0.6	149	24						
Wet	November 2010	8.7	0.7	7.2	0.6	101	24	8.73E+06	1.36E+07	7.28E+05	6.33E+04	89	139
Wet	November 2010	9.3	0.7	7.2	0.6	147	24	5.61E+06	7.87E+06	7.28E+05	6.33E+04	54	76
Wet	November 2010	9.3	0.7	7.6	0.6	111	18	9.45E+06	1.46E+07	7.28E+05	6.33E+04	97	150
Wet	November 2010	10.4	0.7	8.3	0.7	81	13	1.36E+07	2.48E+07	7.28E+05	6.33E+04	144	261
Wet	November 2010	11.3	0.4	10.2	0.7	72	12	1.34E+07	2.14E+07	7.28E+05	6.33E+04	141	225

aquifer and transporting ^{222}Rn through the peat into the surface water flooding the mangrove forest. Radon-222 activity in the groundwater approximately 7 mbls is two to three times greater than the pore water average and thus could contribute to the surface water concentration in the ebb fluxes. However, the path for groundwater discharge is complex and very diffuse. For the same area of SRSE, Whelan et al. (2005) showed that head was higher in the aquifer during the wet season (0.12 m), but the wet season vertical head gradients ($5.4 \times 10^{-2} \text{ m m}^{-1}$, positive upward) were either the same or less than during the dry season ($7.6 \times 10^{-2} \text{ m m}^{-1}$). This suggests that vertical upward seepage is feasible as has been previously indicated (Price et al. 2003; Price et al. 2006); however, this would occur at similar rates year round as the head gradients always favor vertical upward flow. Also, the small creek examined in this study is separated from the underlying aquifer by 5–7 m of low permeability peat deposits (Whelan et al. 2005). Since most of the porosity in the mangrove peat originates from the burrows, the likelihood of a deeper groundwater source seems low, at least for the mangrove forest proper.

The wet season radon activities and salinities are quantitatively less than the dry season. Precipitation leading up (2 weeks; Elec. Supp. Material A1) was similar for the two samplings during the wet seasons (145.3 and 66.5 mm for September and November 2010) but significantly different for the dry season (5.5 mm). Reduced salinity during the ebb and slack low tide also supports an additional freshwater source during the wet season. The added precipitation, if stored as surface water features, could locally dilute the ^{222}Rn and account for lower salinity but would have to be either within a few days prior to the sampling. Somewhat in opposition to this explanation though are the water levels in

the mangrove forest. Water levels observed above the forest floor do not appear to vary seasonally, suggesting that water level in the mangrove forest is strictly tidal modulated. Thus, if meteoric water was to be retained, it would have to be locally stored in small pools. Alternatively, the younger meteoric water could percolate into the mangrove soil increasing soil saturation. Such dynamics in soil saturation would have bearing on the recoil and supply of ^{222}Rn and its ingrowth in the pore fluids as well as the effectiveness of tidal flooding on burrow flushing.

Burrows, Mangrove “Sponge,” and Pathway for Enhanced Respiration

The peat that accumulates in mangrove environments is often considered to have low permeability and a large fluid exchange capacity (Hemond and Fifield 1982; Wilson and Gardner 2006; Xin et al. 2009; Xin et al. 2013). Contributing to this exchange capacity is the abundance of burrows and similar secondary porosity modifications associated with an active benthic infaunal community (Hemond and Fifield 1982; Stieglitz et al. 2000; Koretsky et al. 2002; Gardner and Gaines 2008). The SRSE is one such place where there is limited knowledge on how these modified macroporous structures influence surface water-groundwater exchange. In mangrove ecotones such as the SRSE, dominant crab families include Ocypodidae (fiddler), Xanthidae (mud), and Grapsidae (grapsid). The abundance of these families is variable but the commonality is that they tend to rework sediments and create burrows that link the surface and subsurface environments. The efficiency at which the burrows are flushed during a tidal cycle has a significant impact on material

budgets in these mangrove ecotones (Smith et al. 1991; Gleeson et al. 2013; Maher et al. 2013).

Crab burrow density does not vary along SRSE (i.e., upstream to downstream) nor does it vary inland away from the main channel (Balentine et al. 2008). According to Balentine et al. (2008), burrow density along SRSE ranged from 60 to 110 burrows m^{-2} with a mean of 80 burrows m^{-2} . Assuming a 10,000- m^2 drainage area for the tidal creek at SRS-6, approximately 800,000 burrows are expected to occur within the study area. With a burrow volume of approximately $2.5 \times 10^{-4} \text{ m}^3$ per burrow, that equates to 200 m^3 of total burrow volume that is subject to tidal flushing. The ^{222}Rn mass balance approaches result in volumetric exchange that range from 32 to 250 m^3 per tidal cycle with a mean of 87.6 m^3 . Building upon the evidence of seasonal variability observed, fluid exchange expected during the dry season ($\sim 250 \text{ m}^3$) would flush all the burrows present. In contrast, during the wet season, single tide volumes are on the order of 50–60 m^3 , which would suggest a residence time of 2 days and a burrow flushing efficiency of 25 %. There is only slight variation in pore water ^{222}Rn during the dry and wet season, which suggests that the difference in burrow flushing is controlled by exchange of ^{222}Rn between the peat and burrows. During the wet season, the peat is at saturation (i.e., soil saturation index of 1) due to a combination of tidal inundation and precipitation. The pressure gradient (i.e., loading) between burrow water and flood tide is small (Xin et al. 2009) limiting advective exchange. In contrast, during the dry season, the peat is not fully saturated (i.e., soil saturation index less than 1) and the water that enters the burrows during the flood tide can seep into the surrounding peat matrix. Xin et al. (2009) was able to model this gradient in salt marsh peats, which are comparable in terms of transmissivity and hydrodynamics to the mangrove forest. Modeled pressure gradients showed a net seepage from the burrows to adjacent peat during the flood tide and subsequent drainage during the falling tide. This flooding and drainage process during the dry season would enhance net material exchange.

Normalizing our volumetric flux rates over the entire area of the mangrove forest floor drained by the small creek (10,000 m^2) results in specific groundwater discharge rates that range between 6.7 to 50 $\text{L m}^{-2} \text{ day}^{-1}$. These rates are 3 to 4 orders of magnitude higher than discharge obtained from a temperature-based, 1D advection-conduction model (Spence 2011). The temperature model results, while accounting for variable permeability, do not incorporate macroporous flow, which appears to be the primary pathway for benthic exchange in these mangrove peats. Similarly, the radionuclide-based flux estimates are 7 to 50 times greater than the contribution of fresher groundwater from the confined Biscayne Aquifer as reported by Saha et al. (2011). Again, the water budget approach focuses solely on the freshwater imbalance and does not account for marine groundwater fluxes.

Considering the peat thickness ($\sim 600 \text{ cm}$) and the low hydraulic conductivity of the mangrove peat (18.7 cm day^{-1} ; Whelan et al. 2005), nearly all the discharge implied by the radon budgets would be modified surface water with little contribution from deeper aquifers (e.g., Biscayne). In areas where the peat thickness is greatly reduced (e.g., in channels and upstream), the contribution from both deep aquifer groundwater, whether marine or terrestrial in source, would be more important than at SRS-6. It appears based on the radon budgets that at SRS-6 tidal pumping of crab burrows dominates.

Similar radionuclide-based discharge rates have been reported in the literature for mangrove regions in Australia (e.g., Gleeson et al. 2013; Stieglitz et al. 2013). With the addition of the SRSE observations, an assessment of commonality and distinction among different mangrove systems is possible. Using ^{222}Rn and radium isotopes, Stieglitz et al. (2013) estimate rates of fluid exchange that are on the order of 30.4 $\text{L m}^{-2} \text{ day}^{-1}$. While the two flushing rates are quite comparable, there is considerable variability in the two benthic communities. Based on Stieglitz et al. (2000), the Coral Creek system in Australia is characterized by very few (i.e., 1.8 burrow m^{-2}) yet large (70 L) burrows. In contrast, the SRSE system is characterized by high burrow density with low volumes. This high density, low volume leads to larger water-burrow wall interaction than would large-volume, low-density systems such as Coral Creek.

Variation in flushing efficiency will have a profound impact on organic matter diagenesis and carbon efflux. Previous studies have shown the impact of surface water-groundwater exchange on the transport of material out of the mangrove forest soil but few have noted the potential for enhancing remineralization within the mangrove soil. In other submarine environments, the effects of burrow chemistry on metal and other elemental cycling has been demonstrated and shown to have a significant impact on reduction and oxidation processes (e.g., Klerks et al. 2007; Meysman et al. 2006). Respiration and NO_3^- reduction are more favorable modes for oxidation of organic matter than other terminal electron acceptors. Thus, reduced fluid residence time in the burrows during the dry season would increase the exposure of the organic matter to oxygen and increase oxidation rates through successive tides. Given the large density and abundance of crab burrows in the region, the potential impact on soil elevation is likely. Even with an increase in residence of 0.5 to 2 days, the potential impact on organic matter degradation and subsequent subsidence is an important process still mostly overlooked in this setting. Further studies or advancements to measure actual burrow flushing rates versus apparent burrow flushing rates may help quantitatively verify these results. The enhanced interaction of the water with these burrow walls could result in more complex material exchange and cycling (e.g., organic carbon or mercury; Bergamaschi et al. 2011) and should be the focus of future research.

Groundwater Contributions to the Estuary

Groundwater discharge from the Biscayne Aquifer does not appear to be a likely driver of ^{222}Rn variability at SRS-6 moorings. However, groundwater discharges occurring where parts of the carbonate aquifer are unconfined or exposed (i.e., such as the channel, see later section) cannot be excluded. Previous studies have identified that groundwater is an important pathway for macronutrients in the mangrove ecotone. Price et al. (2003) observed that density-corrected, hydraulic gradients between brackish groundwater and surface water favored groundwater discharge along portions of the FCE-LTER including SRSE. Saha et al. (2011) developed a water budget for this region using hydrologic data spanning 2002–2008 and verified Price et al. (2003) semi-quantitative observations. Based on the water budget, combined fresh groundwater discharge from surficial peat aquifer (0–6 m below land surface) and the underlying aquifer was on the order of 400 mm year^{-1} ($\sim 0.11 \text{ cm day}^{-1}$). Several observations in our data suggest that groundwater into the channel may be significant and more prevalent in the dry season.

Surveys of ^{222}Rn found that surface water activities are lower in the dry season than in the wet season. While ^{222}Rn provided a quantitative tracer for tidal exchange (due to its conservative nature and short half-life), it may not be the best tracer for examining basin-scale groundwater exchange. In this low-gradient system, there are more sources of ^{222}Rn than can be distinguished by simple surface water measurements. As observed in the time series studies, a significant efflux of ^{222}Rn occurs from the mangrove forest soil during each tidal exchange. The daily addition of radon limits its applicability as a quantitative tracer over the basin scale as the end-member concentrations between the deep groundwater and the shallow mangrove pore water are not grossly different (i.e., a factor of 1 to 5) across the estuarine gradient (Table 1). The radium data show promise in evaluating much larger scale dynamics. The variability in the half-lives of the various radium-isotopes may help elucidate mixing, residence time, and groundwater contributions. For example, the low $^{224}\text{Ra}/^{226}\text{Ra}$ activity ratios observed during low-tide and during the dry season are quantitatively similar to the groundwater ratio. This implies that groundwater from the Biscayne Aquifer is more influential to the surface hydrochemistry of the SRSE proper during the dry season when surface water flows are most reduced. In contrast, surface water $^{224}\text{Ra}/^{226}\text{Ra}$ is notably higher during the wet season than the dry season (Table 2). Driving ratio difference though is ^{226}Ra activity, which is much lower in the wet season than the dry. The long half-life of ^{226}Ra would suggest that it is not readily regenerated on tidal time scales and thus would be sourced by a longer flow path than the short-lived isotopes (Rodellas et al. 2015). Thus, groundwater from the Biscayne Aquifer may be the major supplier of the ^{226}Ra and tidal exchange the main input of ^{223}Ra or ^{224}Ra (i.e.,

similar to ^{222}Rn). Therefore, deep groundwater inputs from the Biscayne Aquifer are more readily detectable during the dry season than during the wet season. The source of this groundwater remains unclear to whether it originates as fresh or saline groundwater or if the contribution of these two end-members vary considerable through time in response to hydraulic gradients in the surface estuary.

Unfortunately, the nonconservative behavior of radium is not well characterized for this SRSE with this data set. Radium is an alkaline earth metal is known to have nonconservative behavior in estuarine environments. Classic studies attribute this nonconservative behavior to sorptive processes of suspended particles (e.g., Li and Chan 1979), but more recent studies (e.g., Gonneea et al. 2008) have shown that other processes are influencing radium's behavior in solution. Webster et al. (1994, 1995) showed Ra^{2+} adsorbed onto clay and organics readily desorbed when particles were exposed to higher ionic strength solution, which contain abundant seawater cations such as Na^+ and Ca^{2+} .

In order to provide quantitative estimates of SGD using radium would require estimates of desorption rates and characterization of both the mangrove soil and the carbonate channel (Webster et al. 1995; Rama and Moore 1996; Michael et al. 2011; Stieglitz et al. 2013), but these rates are not available for these sediment. However, the radium isotope data support that geochemically groundwater is more influential in the dry season than in the wet season along the SRSE. Additional work characterizing the potential sources of radium isotopes may help fully elucidate the volumetric contributions of groundwater to the Everglades, whether it is of fresh, brackish, or saline origin.

Conclusions

Attempts to scale up fluid fluxes especially over low hydraulic gradient systems such as coastal mangrove forests are challenging. As shown for the SRSE, temporal variability occurs at both daily and seasonal time scales. Extrapolating one time period to an annual time scale or large spatial scale could neglect significant contributions from mixed tides and variable seasonal fresh, surface water inputs. Based on observations from SRS-6, tidal variations drive a significant material exchange (e.g., radon) between the mangrove forests and the overlying water column by flushing crab burrows. This tidal flushing is responsible for a large outwelling signature of radon from the mangrove forest. In addition to the tidal fluxes, there is an apparent seasonal difference in the radon fluxes exiting the mangrove forest. The wet season observations provide conservatively low estimates of radon exchange while the dry season is nearly four times higher. These seasonal variations may be associated with saturation states of the mangrove soil, where low saturation in the dry season allows for

better exchange between the soil and the burrow water and vice versa in the wet season.

A radon mass balance approach suggest that recirculation or burrow flushing within the mangrove forest is several orders of magnitude greater than previous estimates of groundwater discharge along the SRSE. Such exchange rates must be accounted for in material exchange in these low gradient systems. Additional lateral fluxes can occur through communication between the main river channels and the underlying aquifer. As such, attempts to scale and fully quantify groundwater discharge and fluid exchange and its two primary components requires a substantial assessment of both mangrove outwelling and tidal pumping across the channel as identified in the mapping of radon during both wet and dry seasons as well as the long-lived ^{226}Ra isotope.

Acknowledgments This material is based upon work supported by the National Science Foundation through the Florida Coastal Everglades Long-Term Ecological Research program under Grant Nos. DBI-0620409 and DEB-1237517. This is SERC contribution number 774. The authors would like to thank T.J. Smith, III and Gordon Anderson for access to groundwater wells along the Shark River Slough as well as Jordon Sanford and Lance Thomson for their help in the field. We would also like to think Lisa Robbins and two anonymous reviews for providing constructive feedback that greatly improved the quality of this manuscript. Finally, we would like to thank Victor Engel (formerly of the National Park Service) and the National Park Service for access to the Florida Coastal Everglades. The authors CGS and PWS would like to thank the USGS Coastal and Marine Geology Program for continued support. Any use of trade, product, or firm names is for descriptive purposes only and does not imply endorsement by the US government.

References

- Anderson, M.S., V.N.R. Jakobsen, and D. Postma. 2005. Geochemical processes and solute transport at the seawater/freshwater interface of a sandy aquifer. *Geochimica et Cosmochimica Acta* 69: 3979–3994.
- Badon-Ghyben, W. 1889. Nota in verband met de voorgenomen put boring nabij Amsterdam (notes on the probable results of the proposed well drilling near Amsterdam). Koninkl. Inst. Ing. Tijdschr, 1888-89, *The Hague*: 21.
- Balentine, K.M., G. Tiling, and T.J. Smith III (eds.). 2008. Overview of USGS Coastal and Marine Geology Program data management and analysis tools for geologic and hazards information [abs.], USGS Gulf Coast Science Conference and Florida Integrated Science Center Meeting: Proceedings with abstracts, October 20-23, 2008, 2008–1329. Orlando: U.S. Geological Survey Open-File Report. 96 pp.
- Bergamaschi, B.A., D.P. Krabbenhoft, G.R. Aiken, E. Patino, D.G. Rumbold, and W.H. Orem. 2011. Tidally driven export of dissolved organic carbon, total mercury, and methylmercury from a mangrove-dominated estuary. *Environmental Science & Technology* 46: 1371–1378.
- Berner, R.A. 1980. *Early diagenesis: a theoretical approach*. Princeton: Princeton University Press. 241 pp.
- Boto, K.G., and J.S. Bunt. 1981. Tidal export of particulate organic matter from a Northern Australian mangrove system. *Estuarine, Coastal and Shelf Science* 13: 247–255.
- Breithaupt, J.L., J.M. Smoak, T.J. Smith, C.J. Sanders and A. Hoare. 2012. Organic carbon burial rates in mangrove sediments: Strengthening the global budget. *Global Biogeochemical Cycles* GB3011, doi:10.1029/2012gb004375.
- Burnett, W.C., G. Kim, and D. Lane-Smith. 2001. A continuous monitor for assessment of Rn-222 in the coastal ocean. *Journal of Radioanalytical and Nuclear Chemistry* 249: 167–172.
- Burnett, W.C., P.K. Aggarwal, A. Aureli, H. Bokuniewicz, J.E. Cable, M.A. Charette, E. Kontar, S. Krupa, K.M. Kulkarni, A. Loveless, W.S. Moore, J.A. Oberdorfer, J. Oliveira, N. Ozyurt, P. Povinec, A.M.G. Privitera, R. Rajar, R.T. Ramassur, J. Scholten, T. Stieglitz, M. Taniguchi, and J.V. Turner. 2006. Quantifying submarine groundwater discharge in the coastal zone via multiple methods. *Science of the Total Environment* 367: 498–543.
- Burnett, W.C., I.R. Santos, Y. Weinstein, P.W. Swarzenski, and B. Herut. 2007. Remaining uncertainties in the use of Rn-222 as a quantitative tracer of submarine groundwater discharge. In *A New Focus on Groundwater-Seawater Interactions*, ed. W. Sanford, C. Langevin, M. Polemio, and P. Povinec, 125–133. Perugia: IAHS Publ.
- Cooper, H.H. 1959. A hypothesis concerning the dynamic balance of fresh water and salt water in a coastal aquifer. *Journal of Geophysical Research* 64: 461–467.
- Crusius, J., D. Koopmans, J.F. Bratton, M.A. Charette, K. Kroeger, P. Henderson, L. Ryckman, K. Halloran, and J.A. Colman. 2005. Submarine groundwater discharge to a small estuary estimated from radon and salinity measurements and a box model. *Biogeosciences* 2: 141–157.
- Dittmar, T., and R.J. Lara. 2001. Driving forces behind nutrient and organic matter dynamics in a mangrove tidal creek in north Brazil. *Estuarine, Coastal and Shelf Science* 52: 249–259.
- Dittmar, T., N. Hertkorn, G. Kattner and R.J. Lara. 2006. Mangroves, a major source of dissolved organic carbon to the oceans. *Global Biogeochemical Cycles* GB1012, doi:10.1029/2005gb002570.
- Duever, M.J., J.F. Meeder, L.C. Meeder, and J.M. McCollom. 1994. *The climate of South Florida and its role in shaping the Everglades ecosystem. Everglades—the ecosystem and its restoration: Delray Beach*, 225–248. Florida: St. Lucie Press.
- Dulaiova, H., R. Peterson, W.C. Burnett, and D. Lane-Smith. 2005. A multi-detector continuous monitor for assessment of Rn-222 in the coastal ocean. *Journal of Radioanalytical and Nuclear Chemistry* 263: 361–365.
- Gardner, L.R., and E.F. Gaines. 2008. A method for estimating pore water drainage from marsh soils using rainfall and well records. *Estuarine, Coastal and Shelf Science* 79: 51–58.
- Gleeson, J., I.R. Santos, D.T. Maher, and L. Golsby-Smith. 2013. Groundwater-surface water exchange in a mangrove tidal creek: Evidence from natural geochemical tracers and implications for nutrient budgets. *Marine Chemistry*. doi:10.1016/j.marchem.2013.02.001.
- Gonnea, M.E., P.J. Morris, H. Dulaiova, and M.A. Charette. 2008. New perspectives on radium behavior within a subterranean estuary. *Marine Chemistry* 109: 250–267.
- Hemond, H.F., and J.L. Fifield. 1982. Subsurface flow in salt marsh peat: a model and field study. *Limnology and Oceanography* 27: 126–136.
- Kim, G., and P.W. Swarzenski. 2010. Submarine groundwater discharge (SGD) and associated nutrient fluxes to the coastal ocean. In *Carbon and nutrient fluxes in continental margins*, ed. K.-K. Liu, L. Atkinson, R. Quiñones, and L. Talaue-McManus, 529–538. Heidelberg: Springer Berlin.
- Kim, G., W.C. Burnett, H. Dulaiova, P.W. Swarzenski, and W.S. Moore. 2001. Measurement of ^{224}Ra and ^{226}Ra activities in natural waters using a radon-in-air monitor. *Environmental Science & Technology* 35: 4680–4683.

- Klerks, P.L., D.L. Felder, K. Strasser, and P.W. Swarzenski. 2007. Effects of ghost shrimp on zinc and cadmium in sediments from Tampa Bay, FL. *Marine Chemistry* 104: 17–26.
- Koretsky, C.M., C. Meile, and P. Van Cappellen. 2002. Quantifying bioirrigation using ecological parameters: a stochastic approach. *Geochemical Transactions* 3: 17–30.
- Li, Y.-H., and L.-H. Chan. 1979. Desorption of Ba and ^{226}Ra from river-borne sediments in the Hudson estuary. *Earth and Planetary Science Letters* 43: 343–350.
- Maher, D.T., I.R. Santos, L. Golsby-Smith, J. Gleeson, and B.D. Eyre. 2013. Groundwater-derived dissolved inorganic and organic carbon exports from a mangrove tidal creek: The missing mangrove carbon sink? *Limnology and Oceanography* 58: 475–488.
- Martens, C.S., G.W. Kipphut, and J.V. Klump. 1980. Sediment-water chemical exchange in the coastal zone traced by in situ radon-222 flux measurements. *Science* 208: 285–288.
- Martin, J.B., J.E. Cable, C. Smith, M. Roy, and J. Cherrier. 2007. Magnitudes of submarine groundwater discharge from marine and terrestrial sources: Indian River Lagoon, Florida. *Water Resources Research* W05440. doi:10.1029/2006WR005266.
- Meile, C., and P. Van Cappellen. 2003. Global estimates of enhanced solute transport in marine sediments. *Limnology and Oceanography* 48: 777–786.
- Meysman, F.J.R., E.S. Galaktionov, B. Gribsholt, and J.J. Middelburg. 2006. Bioirrigation in permeable sediments: advective pore-water transport induced by burrow ventilation. *Limnology and Oceanography* 51: 142–156.
- Michael, H.A., A.E. Mulligan, and C.F. Harvey. 2005. Seasonal oscillations in water exchange between aquifers and the coastal ocean. *Nature* 436: 1145–1148.
- Michael, H.A., M.A. Charette, and C.F. Harvey. 2011. Patterns and variability of groundwater flow and radium activity at the coast: a case study from Waquoit Bay, Massachusetts. *Marine Chemistry* 127: 100–114.
- Moore, W.S. 1999. The subterranean estuary: A reaction zone of ground water and sea water. *Marine Chemistry* 65: 111–125.
- Moore, W.S., and R. Arnold. 1996. Measurement of Ra-223 and Ra-224 in coastal waters using a delayed coincidence counter. *Journal of Geophysical Research, Oceans* 101: 1321–1329.
- Moore, W.S., and D.F. Reid. 1973. Extraction of radium from natural-waters using manganese-impregnated acrylic fibers. *Journal of Geophysical Research* 78: 8880–8886.
- Parker, G.G., N.D. Hoy and M.C. Schroeder. 1955. Geology. In *Water resources of Southeastern Florida with Special Reference to Geology and Groundwater of the Miami Areas*, eds. G.G. Parker, G.E. Gerguson, A.J. Love and et al, 1255, 57–125. USGS Water Supply Paper.
- Peterson, R.N., I.R. Santos, and W.C. Burnett. 2009. Evaluating groundwater discharge to tidal rivers based on a Rn-222 time-series approach. *Estuarine, Coastal and Shelf Science* 86: 165–178.
- Price, R.M., Z. Top, J.D. Happell, and P.K. Swart. 2003. Use of tritium and helium to define groundwater flow conditions in Everglades National Park. *Water Resources Research* 39:1267. doi:10.1029/2002WR001929.
- Price, R.M., P.K. Swart, and J.W. Fourqurean. 2006. Coastal groundwater discharge - an additional source of phosphorus for the oligotrophic wetlands of the Everglades. *Hydrobiologia* 569: 23–36.
- Rama, and W.S. Moore. 1996. Using the radium quartet for evaluating groundwater input and water exchange in salt marshes. *Geochimica et Cosmochimica Acta* 60: 4645–4652.
- Robinson, C., L. Li, and D.A. Barry. 2007. Effect of tidal forcing on a subterranean estuary. *Advances in Water Resources* 30: 851–865.
- Rodellas, V., J. Garcia-Orellana, P. Masque, and J.S. Font-Munoz. 2015. The influence of sediment sources on radium-derived estimates of Submarine Groundwater Discharge. *Marine Chemistry* 171: 107–117.
- Roy, M., J.B. Martin, J. Cherrier, J.E. Cable, and C.G. Smith. 2010. Influence of sea level rise on iron diagenesis in an east Florida subterranean estuary. *Geochimica et Cosmochimica Acta* 74: 5560–5573.
- Saha, A.K., C.S. Moses, R.M. Price, V. Engel, T.J. Smith Iii and G. Anderson. 2011. A hydrological budget (2002–2008) for a large subtropical wetland ecosystem indicates marine groundwater discharge accompanies diminished freshwater flow. *Estuaries and Coasts*. doi:10.1007/s12237-011-9454-y.
- Santos, I.R., R.N. Peterson, B.D. Eyre, and W.C. Burnett. 2010. Significant lateral inputs of fresh groundwater into a stratified tropical estuary: evidence from radon and radium isotopes. *Marine Chemistry* 121: 37–48.
- Santos, I.R., B.D. Eyre, and M. Huettel. 2012. The driving forces of porewater and groundwater flow in permeable coastal sediments: a review. *Estuarine, Coastal and Shelf Science* 98: 1–15.
- Schubert, M., A. Paschke, E. Lieberman, and W.C. Burnett. 2012. Air-water partitioning of Rn-222 and its dependence on water temperature and salinity. *Environmental Science & Technology* 46: 3905–3911.
- Smith, C.G., and P.W. Swarzenski. 2012. An investigation of submarine groundwater-borne nutrient fluxes to the west Florida shelf and recurrent harmful algal blooms. *Limnology and Oceanography* 57: 471–485.
- Smith III, T.J., K.G. Boto, S.D. Frusher, and R.L. Giddins. 1991. Keystone species and mangrove forest dynamics: the influence of burrowing by crabs on soil nutrient status and forest productivity. *Estuarine, Coastal and Shelf Science* 33: 419–432.
- Smith, C.G., J.E. Cable, and J.B. Martin. 2008. Episodic high-intensity mixing events in a subterranean estuary: Effects of tropical cyclones. *Limnology and Oceanography* 53: 666–674.
- Spence, V. 2011. Estimating groundwater discharge in the oligohaline ecotone of the Everglades using temperature as a tracer and variable-density groundwater models. Masters Thesis, Department of Geology, University of South Florida, 36 pp.
- Stieglitz, T., P. Ridd, and P. Müller. 2000. Passive irrigation and functional morphology of crustacean burrows in a tropical mangrove swamp. *Hydrobiologia* 421: 69–76.
- Stieglitz, T.C., J.F. Clark, and G.J. Hancock. 2013. The mangrove pump: the tidal flushing of animal burrows in a tropical mangrove forest determined from radionuclide budgets. *Geochimica et Cosmochimica Acta* 102: 12–22.
- Swarzenski, P.W. 2007. U/th series radionuclides as coastal groundwater tracers. *Chemical Reviews* 107: 663–674.
- Swarzenski, P.W., F.W. Simonds, T. Paulson, S. Kruse, and C. Reich. 2007. A geochemical and geophysical examination of submarine groundwater discharge and associated nutrient loading estimates into Lynch Cove, Hood Canal, WA. *Environmental Science & Technology*. doi:10.1021/es070881a.
- Troxler, T.G., J.G. Barr, J.D. Fuentes, V. Engel, G. Anderson, C. Sanchez, D. Lagomasino, R. Price, and S.E. Davis. 2015. Component-specific dynamics of riverine mangrove CO₂ efflux in the Florida Coastal Everglades. *Agricultural and Forest Meteorology*. doi:10.1016/j.agrformet.2014.12.012.
- Wdowski, S., S.H. Hong, A. Mulcan, and B. Brisco. 2013. Remote-sensing monitoring of tide propagation through coastal wetlands. *Oceanography* 26: 64–69.
- Webster, I.T., G.J. Hancock, and A.S. Murray. 1994. Use of radium isotopes to examine pore-water exchange in an estuary. *Limnology and Oceanography* 39: 1917–1927.
- Webster, I.T., G.J. Hancock, and A.S. Murray. 1995. Modelling the effect of salinity on radium desorption from sediments. *Geochimica et Cosmochimica Acta* 59: 2469–2476.
- Whelan, K.R.T., T.J. Smith III, D.R. Cahoon, J.C. Lynch, and G.H. Anderson. 2005. Groundwater control of mangrove surface elevation: Shrink and swell varies with soil depth. *Estuaries* 28: 833–843.

- Wilson, A.M., and L.R. Gardner. 2006. Tidally driven groundwater flow and solute exchange in a marsh: Numerical simulations. *Water Resources Research* 42: W01405. doi:10.1029/2005WR004302.
- Wingard, G.L., C.A. Budet, R.E. Ortiz, J. Hudley, and J.B. Murray. 2006. Descriptions and preliminary report on sediment cores from the southwest coastal area, part II: Collected July 2005, Everglades National Park, Florida, Open-file report 2006-1271. Reston: U.S. Geological Survey.
- Xin, P., G. Jin, L. Li, and D.A. Barry. 2009. Effects of crab burrows on pore water flows in salt marshes. *Advances in Water Resources* 32: 439–449.
- Xin, P., L. Li, and D.A. Barry. 2013. Tidal influence on soil conditions in an intertidal creek-marsh system. *Water Resources Research* 49: 137–150.
- Younger, P.L. 1996. Submarine groundwater discharge. *Nature* 382: 121–122.